

bs-17422R**[Primary Antibody]**

Histone H3.1 Rabbit pAb

Bioss
ANTIBODIES

www.bioss.com.cn

sales@bioss.com.cn

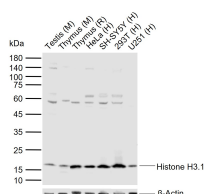
techsupport@bioss.com.cn

400-901-9800

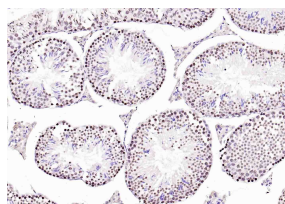
DATASHEET

Host: Rabbit	Isotype: IgG	Applications: WB (1:500-2000) IHC-P (1:100-500) IHC-F (1:100-500) IF (1:100-500) Reactivity: Human, Mouse, Rat (predicted: Rabbit, Pig, Sheep, Cow, Horse, Chimpanzee) Predicted MW.: 15 kDa Subcellular Location: Nucleus
Clonality: Polyclonal		
GeneID: 8350	SWISS: P68431	
Target: Histone H3.1		
Immunogen: KLH conjugated synthetic peptide derived from human Histone H3.1: 71-136/136.		
Purification: affinity purified by Protein A		
Concentration: 1mg/ml		
Storage: 0.01M TBS (pH7.4) with 1% BSA, 0.02% Proclin300 and 50% Glycerol. Shipped at 4°C. Store at -20°C for one year. Avoid repeated freeze/thaw cycles.		
Background: Modulation of the chromatin structure plays an important role in the regulation of transcription in eukaryotes. The nucleosome, made up of four core histone proteins (H2A, H2B, H3 and H4), is the primary building block of chromatin. The N-terminal tail of core histones undergoes different posttranslational modifications including acetylation, phosphorylation and methylation. These modifications occur in response to cell signal stimuli and have a direct effect on gene expression. In most species, the histone H2B is primarily acetylated at lysines 5, 12, 15 and 20. Histone H3 is primarily acetylated at lysines 9, 14, 18 and 23. Acetylation at lysine 9 appears to have a dominant role in histone deposition and chromatin assembly in some organisms. Phosphorylation at Ser10 of histone H3 is tightly correlated with chromosome condensation during both mitosis and meiosis.		

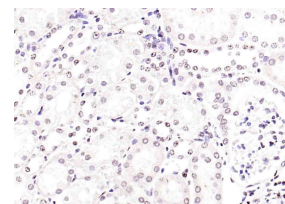
VALIDATION IMAGES



Sample: Lane 1: Mouse Testis tissue lysates Lane 2: Mouse Thymus tissue lysates Lane 3: Rat Thymus tissue lysates Lane 4: Human HeLa cell lysates Lane 5: Human SH-SY5Y cell lysates Lane 6: Human 293T cell lysates Lane 7: Human U251 cell lysates Primary: Anti-Histone H3.1 (bs-17422R) at 1/1000 dilution Secondary: IRDye800CW Goat Anti-Rabbit IgG at 1/20000 dilution Predicted band size: 15 kDa Observed band size: 17 kDa



Paraformaldehyde-fixed, paraffin embedded (mouse testis); Antigen retrieval by boiling in sodium citrate buffer (pH6.0) for 15min; Block endogenous peroxidase by 3% hydrogen peroxide for 20 minutes; Blocking buffer (normal goat serum) at 37°C for 30min; Antibody incubation with (Histone H3.1) Polyclonal Antibody, Unconjugated (bs-17422R) at 1:200 overnight at 4°C, followed by operating according to SP Kit(Rabbit) (sp-0023) instructions and DAB staining.



Paraformaldehyde-fixed, paraffin embedded (mouse kidney); Antigen retrieval by boiling in sodium citrate buffer (pH6.0) for 15min; Block endogenous peroxidase by 3% hydrogen peroxide for 20 minutes; Blocking buffer (normal goat serum) at 37°C for 30min; Antibody incubation with (Histone H3.1) Polyclonal Antibody, Unconjugated (bs-17422R) at 1:200 overnight at 4°C, followed by operating according to SP Kit(Rabbit) (sp-0023) instructions and DAB staining.

SELECTED CITATIONS

- **[IF=16.988]** Wu Yutong. et al. Osteoclast-Derived Apoptotic Bodies Inhibit Naive Cd8 T Cell Activation via Siglec15 Promoting Breast Cancer Secondary Metastasis. Cell Reports Medicine. 2022 Nov 03 WB ;Mouse. 37607544
- **[IF=14.976]** Qinyu Ma. et al. Small extracellular vesicles deliver osteolytic effectors and mediate cancer - induced

Important Note: This product as supplied is intended for research use only, not for use in human, therapeutic or diagnostic applications.

- osteolysis in bone metastatic niche. J Extracell Vesicles. 2021 Feb;10(4):e12068 WB ;Mouse. 33659051
- **[IF=7.5]** Hai-Yi Zhang. et al. Metabolic disruption exacerbates intestinal damage during sleep deprivation by abolishing HIF1 α -mediated repair. CELL REP. 2024 Nov;43: WB ;Mouse. 39527478
 - **[IF=6.953]** Jinshan Wu. et al. Protection by Hosta ventricosa polysaccharides against oxidative damage induced by t-BHP in HepG2 cells via the JNK/Nrf2 pathway. Int J Biol Macromol. 2022 May;208:453 WB ;Human. 35339497
 - **[IF=7.109]** Wu Yutong. et al. Reduced osteoclast-derived apoptotic bodies in bone marrow characterizes the pathological progression of osteoporosis. CELL DEATH DISCOV. 2023 Apr;9(1):1-9 WB ;Mouse. 37185334